A two-step optimisation approach for the design of composite stiffened panels Part I: global structural optimisation

Marco Montemurro, Angela Vincenti, Paolo Vannucci

A two-step optimisation approach for the design of composite stiffened panels
Part I: global structural optimisation

M. Montemurro

Institut d'Alembert UMR7190 CNRS -Université Pierre et Marie Curie Paris 6,
Case 162, 4, Place Jussieu, 75252 Paris Cedex 05, France and
Centre de Recherche Public Henri Tudor, av. 29, J.F. Kennedy, L-1855 Luxembourg-Kirchberg, Luxembourg.

A. Vincenti

Institut d'Alembert UMR7190 CNRS - Université Pierre et Marie Curie Paris 6,
Case 162, 4, Place Jussieu, 75252 Paris Cedex 05, France.

P. Vannucci*

Université de Versailles et St Quentin, 45 Avenue des Etats-Unis, 78035 Versailles, France.

Author for Correspondence:
Paolo Vannucci, Professor,
Université de Versailles et Saint Quentin-en-Yvelines,
45, Avenue des Etats-Unis,
78035 Versailles, France
tel: +33 1 39 25 30 20,
fax: +33 1 39 25 30 15,
e.mail: paolo.vannucci@uvsq.fr

*Corresponding author.

Abstract

This paper deals with the definition of an optimisation procedure for the design of the wing-box composite stiffened panels subject to compression loads. In particular, the objective is to obtain a minimum-weight structure ensuring, at the same time, that the first buckling load should be greater than or equal to a threshold value. The optimisation strategy is subdivided into two phases: in the first one, we perform the global optimisation of the whole structure in terms of geometrical and material design variables, while in the second one the design of the laminate (for both skin and stiffeners laminates) is performed in terms of the stacking sequence. Moreover, no simplifying hypotheses are made on the panel geometry and on the behaviour of the laminates, i.e. types of stacking sequences, which compose the structure and the usual mechanical requirements, such as uncoupling and bending orthotropy, are exactly fulfilled. In this first paper we show the results concerning the first optimisation phase, i.e. the results of the optimisation of the whole wing-box structure. The second phase is detailed in a successive paper.

1 Introduction

Stiffened panels are a structural type extensively used in the aerospace field mainly for their high efficiency: aircraft fuselages, helicopter tails and blades, wing skins, ailerons, flaps and slats represent only few examples.

A deep knowledge of the behaviour of aluminium alloys and the development of accurate analytical models allow to build stiffened panels, made of aluminium alloy, able to work also in the post-buckling field during their life, ensuring in that way a significant reduction of the weight of the whole structure. However, the use of stiffened panels made of composite materials appears to be more convenient in order to have a further substantial reduction of the structural weight: this is mainly due to the high strength-to-weight and stiffness-to-weight ratios of composite materials. Nevertheless, for such kind of structures a complex interaction between experimental and numerical/analytical models is required [1, 2, 3, 4], due to the lack of design procedures. In any case, the design of stiffened composite panels represents one of the major challenges for the aircraft industries. Moreover, experimental studies [5] on the durability of composite stiffened panels, under repeated buckling compression and shear loads, show that, if the composite panels are well designed they are less fatigue sensitive than the metal ones.

Several studies have been conducted on the optimisation of composite stiffened panels subject to buckling and/or strength constraints. A minimum-weight design was performed by Butler and Williams [6] using VICONOPT, a program for buckling and strength analyses based on the direct solutions of the governing equations assuming a sinusoidal law for the deformed shape of the structure. Another minimum-weight design approach, with a constraint on the buckling load, was proposed by Wiggenraad *et al* [7] using the code PANOPT which is based on Riks' derivation for finite-strip analyses. Damage tolerance and soft-skin concepts were introduced to take into account the technological limits on ply thickness and geometry. Nevertheless, the presence of integers or discrete variables, such as the number and the orientation of the layers, number of the stiffeners and so on, makes the use of methaeuristics, in particular genetic algorithms (GAs), more profitable in the optimisation of composite structures [8, 9]. Nagendra *et al* [10] studied the weight-optimisation problem of composite stiffened shells and they found a solution through an improved GA and a finite-strip element method implemented in PASCO, a program used for the evaluation of the buckling load and strain constraints. Kaletta and Wolf [11] used a parallel computing GA to solve the minimum weight design problem of a stiffened composite plate panel, considering constraints on buckling load and maximum strength. They applied this technique using directly a finite element (FE) analysis to evaluate objective and constraint functions. Lillico *et al* [12] studied the problem of the optimal design of the stiffened panel made of aluminium alloy, with constraints on buckling load and post-buckling maximum strength, and solve them through the code VICONOPT. The obtained results were verified using ABAQUS. More recently, Bisagni and Lanzi [13] developed a global approximation strategy in order to find a minimum-weight design for low curvature composite stiffened panel considering, at the same time, the constraints on the buckling load, pre-buckling stiffness and post-buckling collapse load. They developed a neural network system, trained by means of FE analyses, which reproduced the structural response of the whole panel. They used this model, coupled with a standard GA, in order to find the optimal configuration.

The objective of this work is the definition of an optimisation procedure for the design of the wing-box composite stiffened panel subject to compression loads. This strategy was originally conceived for the optimal design of the anisotropy of composite laminated structures with variable stiffness, see [14, 15, 16], and also for multi-physics problems of laminates [17]. In this paper, the goal is to design a minimum weight wing-box structure considering a constraint on the first buckling load. The adopted strategy is subdivided into two phases: the first one concerns the optimisation of the whole structure in terms of geometrical and material design variables, while the second one involves the design of the laminates, for both the skin and the stiffeners, in terms of stacking sequences. This procedure is very general: during the whole process, no simplifying hypotheses are made on the panel geometry and on its mechanical behaviour. Indeed, we have also considered the more general case, i.e. when the wing-box stiffened panel has non-identical stiffeners (in terms of geometrical and material properties) and variable number of stiffeners. In addition, no simplifying hypotheses are formulated on the types of the stacking sequences used for skin and stiffeners laminates: no standard sequences, such as symmetric balanced, angle-ply or cross-ply sequences (typically used in the aeronautical field) are employed. In this manner we have no restriction on the ply's orientation nor on the stack, and in this sense we perform a real global solution search: we show that by renouncing to the use of standard stacking sequences, it is possible to find some wing-box configurations which show a reduction of the weight of the whole structure up to 50% when compared with a classical solution realised by aluminium alloy. Moreover these configurations show good mechanical performances, in terms of pre-buckling stiffness and buckling loads.

Concerning the optimisation tool, a new improved version of the GA BIANCA [18, 19], was employed in both phases of the optimisation procedure. The main difficulty, when dealing with the optimisation of *modular structures*, is how to take into account the variable number of modules, even in the case in which the modules are non-identical, as the case of composite stiffened panels with variable number of stiffeners and non-identical stiffeners. As explained in Sec. 5, in the framework of GAs, this problem corresponds to the search of solutions in a design space made up of individuals with variable number of chromosomes and, hence, belonging to different *species*. For this purpose, we developed new genetic operators that perform the crossover and mutation operations among individuals of different species, see [19]. Moreover, in the first optimisation phase, i.e. the global structural optimisation, BIANCA is coupled with a FE code (ANSYS® in our case) which is used to evaluate the objective and constraint functions, see Sec. 5 and 6.

The paper is organised as follows: firstly the model adopted for the wing-box stiffened panel is described in Sec. 2, then the optimisation strategy is explained in details in Sec. 3. In Sec. 4 we introduce the mathematical background that we need to formulate the global structural optimisation problem, while the main features of the GA BIANCA are presented in Sec. 5. A concise description of the FE model of the wing-box structure is given in Sec. 6 and, finally, in Sec. 7 we show the numerical results of the global structural optimisation.

2 Description of the wing-box section

The optimisation procedure is applied to a classical long-range aircraft wing-box stiffened panel. Fig. 1 shows the conceptual steps which lead to the construction of the approximate model of the wing-box section. In particular, we have considered the wing-box section located at the 60% of the wing span, whose typical dimensions are shown in Fig. 1. These values represent specific dimensions for a long-range aircraft with a design range of about 9300 km (5000 nm), 350 passengers, two engines, cruising altitude between $7620 \div 10668$ m ($25000 \div 35000$ ft) and Mach number of about 0.82. For more details see [20].

The structure has a width w of 2610 mm, height h_b of 720 mm and a length L of 700 mm. The wing-box section represents a portion of the wing between two consecutive ribs. We consider the wing-box simply-supported on these ribs. Fig. 1 shows also the loads acting on the structure in normal flight conditions: in this case, only on the upper panel there can be buckling phenomena. The whole wing-box is made up by composite laminates (both the skin and the stiffeners) with highly anisotropic unidirectional graphite-epoxy layers (T300/5280) [21]. The material properties of the elementary layer are shown in Table 1. Both upper and lower panels have Z-shaped stiffeners with equal flanges. The core and the flanges of each stiffener have the same thickness.

As previously said, no simplifying hypotheses are made on the panel geometry: indeed each stiffener can be different from any other, in terms of geometrical and mechanical behaviour. The only hypothesis concerns the geometry of the whole wing-box section which is symmetric with respect to the global $x - y$ plane, as shown in Fig. 1.

3 Two-step optimisation strategy

When dealing with the problem of the optimal design of *composite modular structures* two main difficulties arise: a) what is the optimal number of repetitive units and b) how to consider the design of the anisotropy of the structure. For this purpose, we have developed an optimisation approach which is subdivided into two steps.

In the first phase, we perform the global structural optimisation of the whole wing-box stiffened panel. In particular, the goal is to find an optimal configuration in terms of geometrical and mechanical parameters. Concerning the mechanical parameters, we consider each laminate that composes the structure (for both the skin and the stiffeners) as an equivalent homogenised plate, whose behaviour is described by a set of elastic invariants, the *polar parameters*. These parameters were originally introduced by Verchery [22] and through these quantities it is possible to express the classical **A**, **B**, **D** tensors which describe the behaviour of the laminate in an effective way for design problems of anisotropic structures. Moreover, the polar parameters are tensor invariants and, hence, they are frame-independent. In addition, we consider quasi-homogeneous, fully-orthotropic laminates, i.e. laminates that are uncoupled and with the same orthotropic elastic behaviour at any direction for bending and extension, see [23, 24]. Through these assumptions, it is possible to reduce the number of polar parameters, and then the number of design variables, which take part in the first phase of the optimisation process. We will describe the role of these parameters in Sec. 4. For more details on the polar formalism the reader is addressed to [25].

In the second phase of the optimisation procedure, we consider the optimal design of the laminates. In particular, the optimal design of the elastic properties of the laminate has been taken into account in this step. This problem can be formulated as the search of one among the absolute minima of a positive semi-definite function of the laminate polar parameters, see [26]. Therefore, the key point of this phase is the construction of the objective function for a quasi-homogeneous, fully-orthotropic laminate having the optimal elastic polar moduli issued from the first step of structural optimisation. In this phase, the design variables are the layers orientations and the optimisation process has to be repeated for the laminates of each stiffener and of the skin.

Despite the adopted procedure is very general and flexible, in the sense that it is possible to extend it to a large number of design cases of modular structures, the number and the nature of design variables involved in the whole process can be quite large and complex. Indeed, we have integer design variables such as the number of stiffeners, discrete variables, e.g. plies orientations, thickness of skin and stiffeners, height of stiffeners, and continuous variables, like the polar parameters of the skin and the stiffeners. The nature of the different design variables and the phase of the optimisation process to which they take part are listed in Table 2.

In the next sections, we describe the mathematical statement of the problem, concerning the first optimisation phase, and we show the optimal configurations found for the global structural optimisation.

4 Formulation of the problem of global structural optimisation

The goal of the global structural optimisation is to find a minimum-weight wing-box section subject to some constraints: we have a constraint on the first buckling load and also existence and feasibility constraints on the polar parameters of each laminate for skin and stiffeners. The optimisation problem is highly non-linear in terms of geometrical and polar parameters. In addition, we include the number of the repetitive units, i.e. the stiffeners, among the design variables: in this manner, depending on the number of stiffeners, the global number of design variables and constraint functions can change for each possible point-solution in the whole design space or, in other words, the procedure determines by itself the optimal number of design variables.

In the following subsections, we describe in details the different kinds of variables involved in the global structural optimisation phase, giving also an idea on the extension of the design space and the nature of some constraint functions.

4.1 Geometrical design variables

Fig. 2 shows the geometrical quantities which describe the repetitive unit of the wing-box stiffened panel. In particular, the geometrical design variables are:

- the number of stiffeners N which can varies from 18 to 23;
- the thickness of each stiffener t_i^S $(i = 1, ..., N)$ which can varies from 2.0 mm to 5.0 mm discretised with a step of 0.125 mm;
- the height of each stiffener h_i^S $(i = 1, ..., N)$ which can varies from 40.0 mm to 90.0 mm discretised with a step of 0.5 mm;
- the thickness of the skin t which can varies from 2.0 mm to 5.0 mm discretised with a step of 0.125 mm.

It can be noticed that the dimension of the design space, and hence the length of the vectors of stiffeners thickness and heights, depends on the number of stiffeners. In addition, for manufacturing reasons, the amplitude of the discretisation step for the thickness of stiffeners and skin corresponds to the elementary layer thickness, as shown in Table 1. Moreover, the width of the flange of each stiffener, d_i^S $(i = 1, ..., N)$, is not a design variable and it depends on the height of the stiffener as shown in Fig. 2. The stiffeners are equispaced with a step b which depends on the number of stiffeners through the following relation:

$$b = \frac{w}{N+1} \ , \tag{1}$$

where w is the width of the whole wing-box section.

4.2 Anisotropic material design variables

As explained in Sec. 3, the polar method gives a representation of any planar tensor by means of its invariants. These invariants are called polar parameters and they have also a physical meaning, i.e. they are directly linked to the different symmetries of the tensor [22, 25].

In the framework of the polar representation it is possible to give a representation of a fourth-order elasticity-like tensor through its invariants, e.g. the reduced stiffness tensor $\mathbf{Q}$ of the lamina can be expressed as:

$$\begin{aligned}
Q_{11} &= \quad T_0 + 2T_1 + R_0\cos 4\Phi_0 + 4R_1\cos 2\Phi_1 \ , \\
Q_{12} &= -T_0 + 2T_1 - R_0\cos 4\Phi_0 \ , \\
Q_{16} &= \quad R_0\sin 4\Phi_0 + 2R_1\sin 2\Phi_1 \ , \\
Q_{22} &= \quad T_0 + 2T_1 + R_0\cos 4\Phi_0 - 4R_1\cos 2\Phi_1 \ , \\
Q_{26} &= -R_0\sin 4\Phi_0 + 2R_1\sin 2\Phi_1 \ , \\
Q_{66} &= \quad T_0 - R_0\cos 4\Phi_0 \ .
\end{aligned} \tag{2}$$

In eqs. (2) the Cartesian components of the ply stiffness tensor $\mathbf{Q}$ are expressed using Voigt's notation. T_0, T_1, R_0, R_1, $\Phi_0 - \Phi_1$ are the polar tensor invariants. T_0 and T_1 are the moduli related to the isotropic part of the tensor, R_0 and R_1 are the moduli related to anisotropic one, while Φ_0 and Φ_1 are the polar angles. For more details on the properties of polar parameters see [25].

In the framework of the Classical Laminated Plate Theory (CLPT), the in-plane, out-of-plane and coupling stiffness tensors, $\mathbf{A}$, $\mathbf{D}$ and $\mathbf{B}$ respectively, can be expressed in terms of the polar parameters:

$$\begin{aligned}
T_0^A, T_0^B, T_0^D &= \frac{1}{m}\sum_{k=1}^{n} T_{0k}\left(z_k^m - z_{k-1}^m\right) , \\
T_1^A, T_1^B, T_1^D &= \frac{1}{m}\sum_{k=1}^{n} T_{1k}\left(z_k^m - z_{k-1}^m\right) , \\
R_0^A e^{4i\Phi_0^A}, R_0^B e^{4i\Phi_0^B}, R_0^D e^{4i\Phi_0^D} &= \frac{1}{m}\sum_{k=1}^{n} R_{0k} e^{4i(\Phi_{0k} + \delta_k)}\left(z_k^m - z_{k-1}^m\right) , \\
R_1^A e^{2i\Phi_1^A}, R_1^B e^{2i\Phi_1^B}, R_1^D e^{2i\Phi_1^D} &= \frac{1}{m}\sum_{k=1}^{n} R_{1k} e^{2i(\Phi_{1k} + \delta_k)}\left(z_k^m - z_{k-1}^m\right) ,
\end{aligned} \tag{3}$$

where T_0^A, T_1^A, R_0^A, R_1^A, Φ_0^A and Φ_1^A are the polar components of tensor $\mathbf{A}$, T_0^B, T_1^B, R_0^B, R_1^B, Φ_0^B and Φ_1^B are the polar components of tensor $\mathbf{B}$, while T_0^D, T_1^D, R_0^D, R_1^D, Φ_0^D and Φ_1^D are the polar components of tensor $\mathbf{D}$. In eqs. (3), m=1,2,3 for the extensional, coupling and bending stiffness tensor, respectively. T_{0k}, T_{1k}, R_{0k}, R_{1k}, Φ_{0k} and Φ_{1k} are the polar parameter of the reduced stiffness tensor of the k^{th} lamina; δ_k is the k^{th} ply's orientation measured with respect to the global frame of the laminate, n is the number of plies, while z_k and z_{k-1} are the z coordinates of the top and bottom k^{th} layer's surfaces. In addition, we remark that expressions (2) are valid for any fourth-order elasticity-like tensor, so it is possible to apply these relations also to the $\mathbf{A}$, $\mathbf{B}$ and $\mathbf{D}$ stiffness tensors of the laminate.

From eqs. (3), it can be noticed that the symmetries of the laminate in terms of extension, coupling or bending behaviour depend on the stacking sequence, i.e. on layer's properties, orientation and thickness as well as the number of plies. When concerned with the design of laminates, a designer has to satisfy at the same time several conditions, including not only common objectives, like for instance buckling load or strength, but also general properties of the elastic response of the laminate, such as uncoupling, extension orthotropy, bending orthotropy and so on. As a matter of fact, it is not easy to take into account all these aspects, and normally designers use some shortcuts to get automatically some properties like uncoupling or extension orthotropy. Vannucci and Vincenti have shown in previous studies (see [18, 26]) that it is possible, in the framework of the polar method, to formulate all the problems of optimal design of laminates including the requirements on elastic symmetries; therefore, a general approach to the design of laminates not affected by simplifying and necessarily limiting assumptions, especially for the design of lightweight structures, is actually possible.

As already said in Sec. 3, in this work we use uncoupled, homogeneous, fully-orthotropic laminates for both the skin and the stiffeners of the wing-box section. Introducing the homogenised stiffness tensors defined as:

$$\begin{aligned} \mathbf{A}^* &= \frac{1}{h_{lam}}\mathbf{A}, \\ \mathbf{B}^* &= \frac{2}{h_{lam}^2}\mathbf{B}, \\ \mathbf{D}^* &= \frac{12}{h_{lam}^3}\mathbf{D}, \end{aligned} \tag{4}$$

the previous conditions on elastic symmetries can be expressed as:

$$\begin{aligned} \mathbf{B}^* &= \mathbf{O} && \textit{uncoupling condition}, \\ \mathbf{A}^* &= \mathbf{D}^* && \textit{homogeneity condition}, \\ \Phi_0^{A^*} - \Phi_1^{A^*} &= K^{A^*}\frac{\pi}{4} && \textit{orthotropy condition}. \end{aligned} \tag{5}$$

If the two first conditions of eqs. (5) are satisfied, the laminate is said *quasi-homogeneous*, see [23, 24]. In eqs. (4) h_{lam} is the global thickness of the laminate, while in eqs. (5) $\Phi_0^{A^*}$ and $\Phi_1^{A^*}$ are the polar angles of the tensor $\mathbf{A}^*$ and K^{A^*} can assume only the values 0 or 1, depending on the shape of orthotropy [25, 26]. Here, we want to remark that, by means of these assumptions, we can use only 6 polar quantities, i.e. $T_0^{A^*}$, $T_1^{A^*}$, K^{A^*}, $R_0^{A^*}$, $R_1^{A^*}$ and $\Phi_1^{A^*}$, instead of 18, in order to describe the behaviour of the laminate (bending parameters are identical to the in-plane ones, whilst coupling components are all zero). Moreover, for the general case of laminates with identical layers, the isotropic moduli $T_0^{A^*}$ and $T_1^{A^*}$ are equal to those of the elementary layer, T_0 and T_1 respectively, see [25]. In addition, as previously said, eqs. (2) are valid for any fourth-order elasticity-like tensor, so for tensor $\mathbf{A}^*$ too. Including the third condition of eqs. (5) into eqs. (2), written for the $\mathbf{A}^*$ tensor, we have that:

$$\begin{aligned} \cos 4\Phi_0^{A^*} &= (-1)^{K^{A^*}} \cos 4\Phi_1^{A^*} \ , \\ \sin 4\Phi_0^{A^*} &= (-1)^{K^{A^*}} \sin 4\Phi_1^{A^*} \ . \end{aligned} \tag{6}$$

Therefore, introducing the quantity $R_{0K}^{A^*} = (-1)^{K^{A^*}} R_0^{A^*}$ (see also [14]), the behaviour of a quasi-homogeneous, fully-orthotropic laminate is described by only 3 parameters: the anisotropic quantities $R_{0K}^{A^*}$, $R_1^{A^*}$ and the polar angle $\Phi_1^{A^*}$ which represents the direction of the orthotropy axis.

Together with the previous remarks, we have to consider some constraints which must be imposed on laminate's polar parameters, see [16]. Firstly, we have some existence constraints, due to the fact that tensors $\mathbf{A}^*$ and $\mathbf{D}^*$ must be positive definite. In particular, for a quasi-homogeneous, fully-orthotropic laminate they can be written as (see [25]):

$$\begin{cases} R_{0K}^{A^*} - T_0^{A^*} \leq 0 \,, \\ 2R_1^{A^*2} - T_1^{A^*}\left[T_0^{A^*} + R_{0K}^{A^*}\right] \leq 0 \,. \end{cases} \tag{7}$$

Besides these conditions, feasibility constraints on laminate's polar parameters must be taken into account. These constraints are due to the fact that, according to CLPT, the anisotropic moduli of the homogenised in-plane and out-of-plane stiffness tensors of the laminate have to be less than or equal to the corresponding anisotropic moduli of the stiffness tensor of the lamina:

$$\begin{cases} -R_0 \leq R_{0K}^{A^*} \leq R_0 \,, \\ 0 \leq R_1^{A^*} \leq R_1 \,. \end{cases} \tag{8}$$

It should be noticed that, by imposing the feasibility constraints of eqs. (8), the first condition of eqs. (7) is automatically satisfied, so it is redundant. Thus, the complete set of feasibility and existence constraints is:

$$\begin{cases} -R_0 \leq R_{0K}^{A^*} \leq R_0 \,, \\ 0 \leq R_1^{A^*} \leq R_1 \,, \\ 2R_1^{A^*2} - T_1^{A^*}\left[T_0^{A^*} + R_{0K}^{A^*}\right] \leq 0 \,. \end{cases} \tag{9}$$

These constraints are to be considered in the search of every laminate composing the skin or the stiffeners of the wing-box section. Finally we remark that, due to the quasi-homogeneity assumption, eqs. (5), the existence and feasibility conditions of eqs. (7) and (8) are automatically valid also for the polar parameters of the tensor $\mathbf{D}^*$, though stated for tensor $\mathbf{A}^*$.

In this work, we used for each laminate highly anisotropic unidirectional graphite-epoxy (T300/5280) laminae, as said in Sec. 2, whose polar parameters assume the following values: $T_0 = 26880$ MPa, $T_1 = 24744$ MPa, $\Phi_0 = \Phi_1 = 0°$, $R_0 = 19710$ MPa and $R_1 = 21433$ MPa.

4.3 Mathematical statement of the problem

As previously said, the goal of the global structural optimisation is to find a minimum-weight wing-box configuration respecting the constraint on buckling load, besides those on existence and feasibility for the polar parameters of the laminates of skin and stiffeners. Therefore, the problem can be stated as follows:

$$
\begin{cases}
\quad\quad\quad\quad\;\; \min\; W\left(t, N, t_i^S, h_i^S\right) & i=1,...,N \quad , \\
\text{subject to :}\;\; p_{cr}\left(t, R_{0K}^{A^*}, R_1^{A^*}, N, t_i^S, h_i^S, (R_{0K}^{A^*})_i^S, (R_1^{A^*})_i^S\right) \geq p_{ref} & i=1,...,N \quad , \\
\quad\quad\quad\quad\;\; -R_0 \leq R_{0K}^{A^*} \leq R_0 & \quad\quad , \\
\quad\quad\quad\quad\;\; 0 \leq R_1^{A^*} \leq R_1 & \quad\quad , \\
\quad\quad\quad\quad\;\; 2{R_1^{A^*}}^2 - T_1^{A^*}\left[T_0^{A^*} + R_{0K}^{A^*}\right] \leq 0 & \quad\quad , \\
\quad\quad\quad\quad\;\; -R_0 \leq (R_{0K}^{A^*})_i^S \leq R_0 & i=1,...,N \quad , \\
\quad\quad\quad\quad\;\; 0 \leq (R_1^{A^*})_i^S \leq R_1 & i=1,...,N \quad , \\
\quad\quad\quad\quad\;\; 2({R_1^{A^*}}^2)_i^S - (T_1^{A^*})_i^S\left[(T_0^{A^*})_i^S + (R_{0K}^{A^*})_i^S\right] \leq 0 & i=1,...,N \quad .
\end{cases}
\tag{10}
$$

In eqs. (10) apex S stand for stiffeners. The quantities without this apex are referred to the skin. p_{ref} is a reference value for the buckling load of the structure. In addition, we have fixed *a priori* the orthotropy direction (for both skin and stiffeners laminates) choosing $\Phi_1^{A^*} = (\Phi_1^{A^*})_i^S = 0,\ (i = 1, ..., N)$, which means that the orthotropy axis of each laminate is aligned with the global x axis of the whole wing-box section, as shown in Fig. 1.

As conclusive remark, it should be noticed that, depending on the number N of stiffeners, the dimension of the design space, and hence the number of design variables, as well as the number of constraint equations can change: in particular the total number of design variables is $4N + 4$, while the total number of constraint equations is $3N + 4$.

5 The improved genetic algorithm BIANCA

The optimisation of engineering modular systems is a difficult task since it implies the optimisation of each constitutive module composing the system, as well as the optimisation of the number of constitutive modules. This is a key-point when dealing with weight optimisation of modular structures, such as the optimisation problem expressed by eqs. (10). As a matter of fact, the number of constitutive modules is an integer value and the design space of such optimisation problems is therefore populated by points representing structures composed of different numbers of modules. As a consequence, the number of constitutive parameters (variables of the optimisation problem) is different for distinct points and the associated mathematical optimisation problem is defined over a design space of variable dimension.

Classical deterministic, descent or gradient-based methods are not suited for such problems, due to their discrete nature and a sound alternative is to apply genetic or evolutionary strategies [27, 28]. On one hand, genetic algorithms (GAs) are naturally adapted to deal with different types of variables (continuous, discrete or pointers; see for instance [18]), and therefore they can treat very easily the number of constitutive modules as a discrete design variable. In addition, GAs are "zero-order" methods, i.e. they do not need the calculation of derivatives to perform the optimisation process, so they are well suited for discrete-valued problems. Finally, vectors of different dimensions can be compared within a GA on the basis of their objective function's value.

According to the metaphor adopted by GAs, each point in the design space corresponds to an individual and its genetic structure is composed of chromosomes and genes [27, 28]. When the object of the optimisation problem is a modular system, each constitutive module is represented by a chromosome, and each chromosome is composed of genes, each one coding a design variable related to the module. In agreement with the paradigms of natural sciences, individuals characterised by different number of chromosomes, i.e. modular structures composed of different number of modules, belong to different species.

In this work, we use the new version of the GA BIANCA, see [18, 19] able to cross individuals belonging to different species. BIANCA is written in FORTRAN language. It is substantially constructed on a classical scheme of standard GAs, see Fig. 3, and based on the Darwinian evolution of species, but it shows however several original features (see [18] for more details). One of its main features is the representation of the information, which is particularly rich and detailed, though non redundant. Moreover, the information restrained in the population is treated in such a way to allow for a deep mixing of the individual genotype. In fact, the reproduction operators, i.e. cross-over and mutation, act on every single gene of the individuals, so allowing for a true independent evolution of each design variable. In BIANCA, an individual is represented by an array of dimensions $n_{chrom} \times n_{gene}$. The number of rows, n_{chrom}, is the number of chromosomes, while the number of columns, n_{gene}, is the number of genes. Basically, each design variable is coded in the form of a gene, and its meaning is linked to both the position and the value of the gene within the chromosome.

In order to deal with optimisation problems for modular structures and hence with optimisation processes involving evolution not only of the individuals, but of the species too, the structure of the individual and, consequently, the representation of the information, as well as the reproduction operators of cross-over and mutation, were modified: details on the new genetic operators that we have introduced in BIANCA are given in [19]. Fig. 4 shows the genotype of the generic r^{th} individual for the optimisation problem of the wing-box structure. This individual has n_r+1 chromosomes. The first chromosome is composed by 3 genes representing the design variables for the skin, i.e. thickness and polar parameters. Chromosomes from 2 to n_r+1 contain 4 genes which are the design variables for each stiffener: geometrical parameters, i.e. thickness and height, as well as the polar parameters. An exception is chromosome 2 that has 5 genes: the fifth additional gene codes the number of modules, i.e. for our problem the number of stiffeners. Letter e stands for empty location. More details on the structure of the individuals and on the operators which perform the crossover among different species can be found in [19].

The constrained minimisation problem, formulated in eqs. (10), is transformed into an unconstrained one defining the penalised objective function as:

$$W_p(\mathbf{x}) = W(\mathbf{x}) + \sum_{k=1}^{q} c_k G_k(\mathbf{x}) \ , \tag{11}$$

where W_p is the penalised weight of the wing-box structure, W is the unpenalised weight, while $\mathbf{x}$ is the vector of design variables. G_k is the k^{th} constraint, q is the total number of constraints, whilst c_k is the k^{th} penalisation coefficient. The constrained minimisation problem is treated by BIANCA according to a classical penalisation scheme. The difficult choice of penalisation coefficients has not to be treated by the engineer because an original method was developed in BIANCA for this purpose, which is called *Automatic Dynamic Penalisation* (ADP) method, for more details see [18].

In addition, for every individual at each generation, the evaluation of the objective and constraint functions is performed via a FE analysis. Hence, we need to couple the GA BIANCA with a FE code: to this purpose we have developed an interface with external software within BIANCA, see [19]. The structure of this interface is shown in Fig. 3.

6 Finite element model of the wing-box section

The finite element analysis is used in order to evaluate the objective and constraint functions for each individual, i.e. for each point solution, in the design space at the current generation. The FE model is built in ANSYS® environment. The need to analyse, within the same generation, different geometrical configurations requires the creation of an ad-hoc input file for ANSYS®, that has to be interfaced with BIANCA, according to the scheme shown in Fig. 3.

Fig. 5 shows the geometry, mesh, loads and boundary conditions of the wing-box FE model. The structure is modelled using SHELL99 elements, with 8 nodes and 6 degrees of freedom (DOFs) per node. This kind of element is well suited for linear and non-linear buckling analyses. Moreover, these shell elements present 3 integration points along the thickness for each ply. It is possible to use them in order to define the laminate in explicit or implicit way: through the explicit definition it is possible to define the laminate directly with the stacking sequence, i.e. plies materials, orientations and thickness, whilst via the implicit definition we define the laminate by means of the classical **A**, **D** and **B** stiffness tensors. Since in the global structural optimisation phase we use the polar parameters in order to characterise the behaviour of each laminate of skin and stiffeners, we use the implicit definition of SHELL99 elements to define the mechanical properties of each laminate.

The wing box is considered simply supported at its terminal sections on two wing ribs. The upper panel is subject to a uniform compression unit force per unit length, while the lower one is subject to a uniform tensile unit force per unit length. Under such kind of loads, which are representative of the loads that the structural elements of the wing-box undergo in normal flight conditions, only the upper panel and the corresponding stiffeners can undergo compression instability phenomena. Both upper and lower panels have N stiffeners with Z-shape section. A linear elastic behaviour has been considered as constitutive material law.

After a preliminary mesh sensitivity study the average dimensions of the shell elements are chosen equal to 14×14 mm^2. The number of shell elements in the whole wing-box structure can vary from 14080 to 17680 depending on the number of stiffeners N, whilst the number of DOFs of the whole model can vary from 270744 to 340164. For each individual/point solution in the design space, an eigenvalue linear buckling analysis is performed in order to evaluate the first buckling load of the structure.

Concerning the optimisation problem of eqs. (10), in order to establish a correct reference value of the first buckling load for all the simulations, i.e. p_{ref}, a first buckling analysis on a reference wing-box section model has to be performed. We have already specified in Sec. 2 the type of wing-box section considered here. The reference wing-box stiffened panels are made by Al-7075-T6 alloy with Young's modulus E of 72395 MPa, Poisson's ratio ν of 0.33, yield stress σ_y of 475 MPa and density ρ of 2.76×10^{-6} kg/mm^3. Concerning the geometrical properties, the whole wing box has the global dimensions shown in Fig. 1, while the upper and lower panels are made by 20 identical stiffeners having the following dimensions: $t^S = 2.96$ mm and $h^S = 62.33$ mm for stiffeners thickness and height, respectively, and $t = 4.93$ mm for skin thickness. The reference value of the first buckling load and of the wing-box section weight are the outcome of this first simulation: their values are $p_{ref} = 1928$ N/mm and $W_{ref} = 1222.62$ N respectively.

7 Numerical results

The design variables, their nature and bounds for the optimisation problem (10) are detailed in Table 3. For our optimisation problem we performed three kinds of simulations. In the first one, the stiffeners are identical, i.e. they have the same value of thickness t^S, height h^S as well as the same values of laminate polar parameters, i.e $(R_{0K}^{A^*})^S$ and $(R_1^{A^*})^S$. Therefore, in this case, we have 8 design variables: the number of stiffeners N, geometrical and polar parameters for stiffeners, i.e. t^S, h^S, $(R_{0K}^{A^*})^S$, $(R_1^{A^*})^S$ and geometrical and polar parameters for skin, i.e. t, $R_{0K}^{A^*}$, $R_1^{A^*}$. In addition, for this first case, the total number of constraints, which appear in eqs. (10), is 7: 1 constraint on the buckling load, 4 feasibility constraints and 2 existence constraints for skin and stiffener polar parameters.

In the second case, we consider the problem of the minimum weight for the wing-box stiffened panel in the most general case, i.e. with non-identical stiffeners. The total number of design variables depends on the number of stiffeners N, as explained in Sec. 4, and can vary between 76 and 96. Moreover, also the number of constraint equations is variable along with the number of stiffeners: the minimum number of constraint equations is 58, while the maximum number is 73.

In the third case, we still consider the problem of the minimum weight for the wing-box stiffened panel with non-identical stiffeners. Nevertheless in this last case, for obvious mechanical reasons, we assume that the whole wing-box section has a symmetric distribution of the geometrical and polar parameters for the stiffeners with respect to the $x - z$ plane of the global reference system, see Fig. 1. With this assumption the total number of design variables and constraint equations is considerably reduced and can vary between 40 and 52 for the design variable, and among 31 and 40 for constraint equations.

7.1 Wing-box panel with identical stiffeners

In this first case, since the stiffeners are identical, the genetic operators that perform the cross-over between different species are no longer required. In this case the structure of the individual is organised as follow: the genotype is made up by only one chromosome with 8 genes: the first gene represents the number of stiffeners N, the genes from 2 to 4 represent the skin design variables, i.e. t, $R_{0K}^{A^*}$ and $R_1^{A^*}$, while the last 4 genes represent the stiffeners design variables, i.e. t^S, h^S, $(R_{0K}^{A^*})^S$ and $(R_1^{A^*})^S$.

Concerning the genetic parameters, the population size is set to $N_{ind} = 50$ and the maximum number of generations is assumed equal to $N_{gen} = 80$. The crossover and mutation probability are $p_{cross} = 0.85$ and $p_{mut} = 1/N_{ind}$, respectively. Selection is performed by roulette-wheel operator and the elitism is active. The ADP method for handling constraints is used.

The best solution found by BIANCA is shown in Table 4. The optimal number of the stiffeners for the weight minimization is 22. The buckling load and the wing-box weight are $p_{cr} = 1943$ N/mm and $W = 587.28$ N respectively. Fig. 6 shows the deformed shape of the structure when the applied load is equal to p_{cr}: we can see that, during the instability phenomenon, the wing-box section is characterised by a local skin buckling among the stiffeners. From Table 4, it can be noticed that the mechanical behaviour is different between skin and stiffeners laminates: despite these laminates are both quasi-homogeneous, fully-orthotropic, the stiffeners laminates are orthotropic with $(K^{A^*})^S = 1$, indeed the value of $(R_{0K}^{A^*})^S$ is negative, while the skin laminate is orthotropic with $K^{A^*} = 0$, i.e. the value of $R_{0K}^{A^*}$ is positive. The global constrained minimum was found after 32 generations, see Fig. 7. This solution shows a reduction of the weight of the whole structure of about 52%, when compared to the reference solution, for a slightly increased buckling load (the solution found is practically on the boundary of the feasible domain, $p_{cr} \simeq p_{ref}$).

7.2 Wing-box panel with non-identical stiffeners

Since the number of stiffeners is variable along with the fact that they are non identical, a cross-over between species is required and the optimal value of N is an outcome of the biological selection: the most adapted species automatically issues as a natural result of the Darwinian selection. As previously said, the number of design variables is $4N + 4$, while the total number of constraint equations is $3N + 4$. The structure of the generic individual-panel is the one discussed in Sec. 5 and shown in Fig. 4.

Concerning the genetic parameters, the population size is $N_{ind} = 70$ and the maximum number of generations is $N_{gen} = 80$. The crossover and mutation probability are still $p_{cross} = 0.85$ and $p_{mut} = 1/N_{ind}$, while the shift operator and chromosomes number mutation probability are $p_{shift} = 0.5$ and $(p_{mut})_{chrom} = (n_{chrommax} - n_{chrommin})/N_{ind}$. Once again, selection is performed by roulette-wheel operator, the elitism is active and ADP method for handling constraints has been used.

The best solution found by BIANCA is shown in Table 5. The optimal number of stiffeners for the weight minimization is 23. The buckling load and the wing-box weight are $p_{cr} = 1931$ N/mm and $W = 620.19$ N respectively. Fig. 8 shows the deformed shape of the structure when the applied load is equal to p_{cr}: we can see that, during the instability phenomenon, the wing-box section is characterised by a local skin buckling among the stiffeners in the region where the stiffeners are less stiff, i.e. the buckling phenomenon occurs in the portion of the upper panel where the stiffeners have the worst combination of geometrical and material design variables. From Table 5, it can be noticed that the mechanical behaviour is different among stiffeners laminates: despite every laminate is quasi-homogeneous, fully-orthotropic, there are some orthotropic laminates with $(K^{A^*})^S = 1$ and others with $(K^{A^*})^S = 0$. The global constrained minimum has been found after 57 generations, see Fig. 9. This solution shows a reduction of the weight of the whole structure of about 49%, when compared to the reference solution, for a slightly increased buckling load (the solution found is practically on the boundary of the feasible domain, $p_{cr} \simeq p_{ref}$).

7.3 Wing-box panel with identical stiffeners, symmetric distribution

In this last case, as said previously, we consider a wing-box section with symmetric distribution of the geometrical and polar parameters for the stiffeners with respect to the $x - z$ plane of the global reference system, see Fig. 1. In this case the total number of design variables can vary between 40 and 52, whilst the number of constraint equations can vary among 31 and 40. The structure of the generic individual-panel is the one discussed in Sec. 5 and shown in Fig. 4.

Concerning the genetic parameters, they are strictly those already used in the previous case.

The best solution found by BIANCA is shown in Table 6. The optimal number of stiffeners for the weight minimization is 22. The buckling load and the wing-box weight are $p_{cr} = 1933$ N/mm and $W = 619.26$ N respectively. Fig. 10 shows the deformed shape of the structure when the applied load is equal to p_{cr}. Despite this solution has a symmetric distribution of the geometrical and polar parameters of the stiffeners, we can see that, during the instability phenomenon, the wing-box section is characterised by an asymmetric local skin buckling, which occurs among the stiffeners in the region where the stiffeners are less stiff. This is due to the fact that the structure is not properly symmetric (in the geometrical sense) and consequently the buckling deformed shape is not symmetric, too. As the previous case, the buckling phenomenon occurs in the portion of the upper panel where the stiffeners have the worst combination of geometrical and material design variables. From Table 6, it can be noticed that the mechanical behaviour is different among stiffeners laminates: despite every laminate is quasi-homogeneous, fully-orthotropic, there are some orthotropic laminates with $(K^{A^*})^S = 1$ and others with $(K^{A^*})^S = 0$. The global constrained minimum has been found after 78 generations, see Fig. 11. This solution shows a reduction of the weight of the whole structure of about 49%, when compared to the reference solution, for a slightly increased buckling load (the solution found is practically on the boundary of the feasible domain, $p_{cr} \simeq p_{ref}$).

8 Conclusions

A two-step procedure for the design of wing-box composite stiffened panels has been presented. The procedure is divided into two phases: the global structural optimisation and the laminate design. In this paper we have shown the results concerning the first phase.

Due to the presence of integer and discrete variables, like the number of stiffeners or the skin and stiffeners geometrical parameters, the use of improved genetic algorithms appears to be particularly profitable. In particular, the use of the GA BIANCA (which is able to cross individual belonging to different species) coupled directly with the FE model results very convenient when dealing with constrained optimisation problems of modular structure, as the one presented in this work. Indeed, in this first phase, we have found some wing-box configurations which show a reduction of the weight of the whole structure up to 50% when compared with a classical solution realised by aluminium alloy.

The proposed approach appears to be very flexible and applicable to various engineering problems in which the results are given by complex and expensive models and a high number of analyses is necessary to reach a suitable optimum. Moreover, the procedure has a high level of versatility: more constraints could be easily added to the optimisation problem, e.g. constraints on the strength, yielding or de-lamination of the laminates which compose the structure, without reducing the power and the robustness of the proposed approach.

Acknowledgements

First author is supported by FNR through Aides à la Formation Recherche Grant PHD-09-139.

References

[1] G. Romeo and G. Frulla. Post buckling behaviour of graphite/epoxy stiffened panels with initial imperfections subjected to eccentric biaxial compression loading. *International Journal of Non-Linear Mechanics*, 32(6):1017–1033, 1997.

[2] C. Bisagni. Numerical analysis and experimental correlation of composite shell buckling and post-buckling. *Composites: Part B*, 31:655–667, 2000.

[3] H-R. Meyer-Piening, M. Farshad, B. Geier, and R. Zimmermann. Buckling loads of CFRP composite cylinders under combined axial and torsion loading-experiments and computations. *Computers and Structures*, 53:427–435, 2001.

[4] O. Park, R.T. Hatfka, B.V. Sankar, Jr. J.H. Starnes, and S. Nagendra. Analytical-experimental correlation for a stiffened composite panel loaded in axial compression. *Journal of Aircraft*, 38(2):379–387, 2001.

[5] T. Weller and J. Singer. Durability of stiffened composite panels under repeated buckling. *International Journal of Solids and Structures*, 26(9):1037–1069, 1990.

[6] R. Butler and F.W. Williams. Optimum design using VICONOPT, a buckling and strength constraint program for prismatic assemblies of anisotropic plates. *Computers and Structures*, 43(4):699–708, 1992.

[7] J.F.M. Wiggenraad, P. Arendsen, and J.M. da Silva Pereira. Design optimisation of stiffened composite panels with buckling and damage tolerance constraints. *American Institute of Aeronautics and Astronautics, AIAA-98-1750*, pages 420–430, 1998.

[8] A. Muc and W. Gurba. Genetic algorithms and finite element analysis in optimization of composite structures. *Computers and Structures*, 54:275–281, 2001.

[9] P.Y. Tabakov. Multi-dimensional optimisation of laminated structures using an improved genetic algorithm. *Computers and Structures*, 54, 1992.

[10] S. Nagendra, D. Jestin, Z. Gürdal, R.T. Hatfka, and L.T. Watson. Improved genetic algorithm for the design of stiffened composite panels. *Computers and Structures*, 58(3):543–555, 1996.

[11] P. Kaletta and K. Wolf. Optimisation of composite aircraft panels using evolutionary computation methods. *Proceedings of ICAS 2000 Congress, Harrogate, UK, 27 August-1 September*, pages 441.1–10, 2000.

[12] M. Lillico, R. Butler, G.W. Hunt, A. Watson, D. Kennedy, and F.W. Williams. Optimum design and testing of a post-buckled stiffened panel. *American Institute of Aeronautics and Astronautics, AIAA-2000-1659*, pages 1–10, 2000.

[13] C. Bisagni and L. Lanzi. Post-buckling optimisation of composite stiffened panels using neural networks. *Composite Structures*, 58:237–247, 2002.

[14] C. Julien. *Conception optimale de l'anisotropie dans les structures stratifiées à rigidité variable par la mèthode polaire-génétiques*. PhD thesis, Institut d'Alembert UMR7190 CNRS -Université Pierre et Marie Curie Paris 6 , France, 2010 (in French).

[15] A. Jibawy, C. Julien, B. Desmorat, A. Vincenti, and F. Léné. Hierarchical structural optimization of laminated plates using polar representation. *International Journal of Solids and Structures*, 48:2576–2584, 2011.

[16] A. Vincenti and B. Desmorat. Optimal orthotropy for minimum elastic energy by the polar method. *Journal of Elasticity*, 102(1):55–78, 2010.

[17] P. Vannucci. A new general approach for optimising the performances of smart laminates. *Mechanics of Advanced Materials and Structures*, in press, 2011.

[18] A. Vincenti, M.R. Ahmadian, and P. Vannucci. BIANCA: a genetic algorithm to solve hard combinatorial optimisation problems in engineering. *Journal of Global Optimisation*, 48:399–421, 2010.

[19] M. Montemurro, P. Vannucci, and A. Vincenti. A genetic algorithm with crossover on species for structural optimisation. *Computers and Structures*, 2011(Submitted).

[20] D.P. Raymer. *Aircraft Design: A Conceptual Approach.* AIAA Education Series, 2006.

[21] S.W. Tsai and T. Hahn. *Introduction to composite materials.* Technomic, 1980.

[22] G. Verchery. Les invariants des tenseurs d'ordre 4 du type de l'élasticité. *Proc. of colloque Euromech 115, VIllard-de-Lans, (France)*, 1979.

[23] P. Vannucci and G. Verchery. Stiffness design of laminates using the polar method. *International Journal of Solids and Structures*, 38:9281–9294, 2001.

[24] E. Valot and P. Vannucci. Some exact solutions for fully orthotropic laminates. *Composite Structures*, 40:437–454, 2005.

[25] P. Vannucci. Plane anisotropy by the polar method. *Meccanica*, 40:437–454, 2005.

[26] P. Vannucci. Designing the elastic properties of laminates as an optimisation problem: a unified approach based on polar tensor invariants. *Structural and Multidisciplinary Optimisation*, 31(5):378–387, 2006.

[27] D.E. Goldberg. *Genetic algorithms.* New York: Addison and Wesley, 1994.

[28] Z. Michalewicz. *Genetic algorithms + data structures = evolutionary programming.* Berlin: Springer, 1994.

Tables

Young's modulus E_1 [MPa]	181000
Young's modulus E_2 [MPa]	10300
Shear modulus G_{12} [MPa]	7170
Poisson's ratio ν_{12}	0.28
Density ρ [kg/mm^3]	1.58×10^{-6}
Ply thickness t_{ply} [mm]	0.125

Table 1: Material properties for unidirectional graphite/epoxy ply T300/5208

Type and nature of design variable	Optimisation phase
Number of stiffeners (integer)	Step 1
Thickness of the skin (discrete)	Step 1
Thickness and height of the stiffeners (discrete)	Step 1
Polar parameters of skin (continuous)	Step 1
Polar parameters of stiffeners (continuous)	Step 1
Orientations of plies for skin laminate (discrete)	Step 2
Orientations of plies for stiffeners laminates (discrete)	Step 2

Table 2: Design variables of the whole optimisation process

Design variable	Type	Lower bound	Upper Bound	Discretisation Step
N	discrete	18	23	1
t_i^S [mm]	discrete	2.0	5.0	0.125
h_i^S [mm]	discrete	40.0	90.0	0.5
$(R_{0K}^{A^*})_i^S$ [MPa]	continuous	-19710.0	19710.0	–
$(R_1^{A^*})_i^S$ [MPa]	continuous	0.0	21433.0	–
t [mm]	discrete	2.0	5.0	0.125
$(R_{0K}^{A^*})$ [MPa]	continuous	-19710.0	19710.0	–
$(R_1^{A^*})$ [MPa]	continuous	0.0	21433.0	–

Table 3: Design variables for the optimisation problem (10).

Design variable	Value
N	22
t^S [mm]	3.625
h^S [mm]	40.0
$(R_{0K}^{A^*})^S$ [MPa]	-984.36
$(R_1^{A^*})^S$ [MPa]	6425.22
t [mm]	4.0
$R_{0K}^{A^*}$ [MPa]	16399.8
$R_1^{A^*}$ [MPa]	1293.26

Table 4: Best values of design variables found using BIANCA for the wing-box FE model, case with identical stiffeners.

Stiffeners				
ID	t^S [mm]	h^S [mm]	$(R_{0K}^{A^*})^S$ [MPa]	$(R_1^{A^*})^S$ [MPa]
01	2.75	86.5	-7336.27	13651.0
02	4.75	55.5	-9565.0	1970.67
03	2.625	55.0	-1392.96	15991.2
04	2.125	73.5	18888.6	14574.8
05	3.625	46.0	-5404.69	2750.73
06	4.625	49.0	5701.86	13261.0
07	2.125	58.0	5924.73	11249.3
08	2.0	65.0	-8450.64	8847.51
09	4.0	48.0	14876.8	4495.6
10	4.0	43.0	-1578.69	739.0
11	3.0	43.5	1801.56	7574.78
12	3.75	41.5	8042.03	4290.32
13	3.0	59.0	-1095.8	11495.6
14	4.25	52.0	17811.3	1149.56
15	4.375	54.0	10865.1	2832.84
16	4.0	84.0	12536.7	13178.9
17	2.125	48.5	3993.16	10633.4
18	3.125	48.5	12276.6	14349.0
19	3.0	56.0	12610.9	11536.7
20	2.125	56.5	-6333.33	7615.84
21	4.375	43.0	15322.6	8950.15
22	3.375	56.0	17551.3	5994.13
23	3.625	41.0	13242.4	7020.53
Skin				
	t [mm]		$R_{0K}^{A^*}$ [MPa]	$R_1^{A^*}$ [MPa]
	4.0		12945.3	882.70

Table 5: Best values of design variables found using BIANCA for the wing-box FE model, case with non-identical stiffeners.

Stiffeners				
ID	t^S [mm]	h^S [mm]	$(R_{0K}^{A^*})^S$ [MPa]	$(R_1^{A^*})^S$ [MPa]
01	4.0	40.0	−10642.20	5850.44
02	2.375	45.0	−5999.02	9648.09
03	4.875	46.5	−3101.66	4844.57
04	2.0	57.0	650.049	14266.9
05	4.25	42.0	16102.6	8211.14
06	2.5	63.0	−1578.69	11557.2
07	4.125	82.5	17477.0	4741.94
08	2.625	55.5	−16437.0	7102.64
09	3.25	52.5	−2990.22	13363.6
10	4.75	53.5	−2581.62	6343.11
11	4.625	43.5	15619.7	11228.7
12	4.625	43.5	15619.7	11228.7
13	4.75	53.5	−2581.62	6343.11
14	3.25	52.5	−2990.22	13363.6
15	2.625	55.5	−16437.0	7102.64
16	4.125	82.5	17477.0	4741.94
17	2.5	63.0	−1578.69	11557.2
18	4.25	42.0	16102.6	8211.14
19	2.0	57.0	650.049	14266.9
20	4.875	46.5	−3101.66	4844.57
21	2.375	45.0	−5999.02	9648.09
22	4.0	40.0	−10642.20	5850.44
Skin				
	t [mm]		$R_{0K}^{A^*}$ [MPa]	$R_1^{A^*}$ [MPa]
	4.0		9527.86	205.279

Table 6: Best values of design variables found using BIANCA for the wing-box FE model, case with non-identical stiffeners with symmetric distribution.

Figures

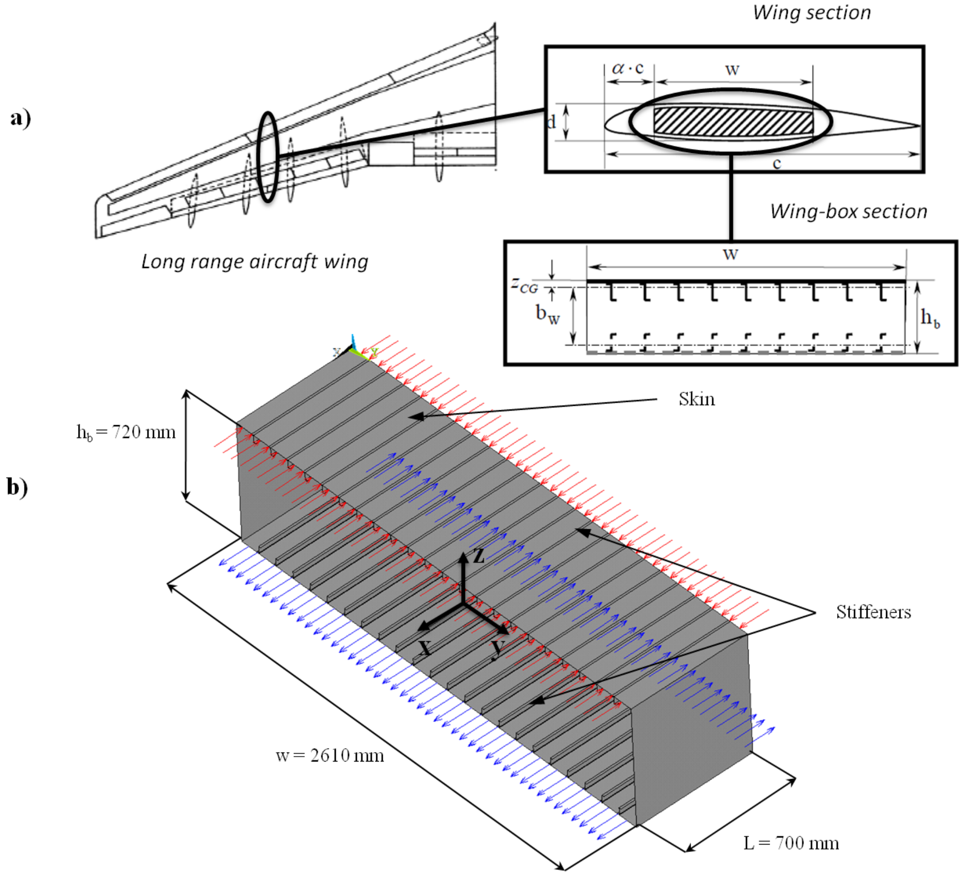

Figure 1: (a) Conceptual phases which lead to the construction of the wing-box model (b) Structure of the wing-box stiffened panel and applied loads.

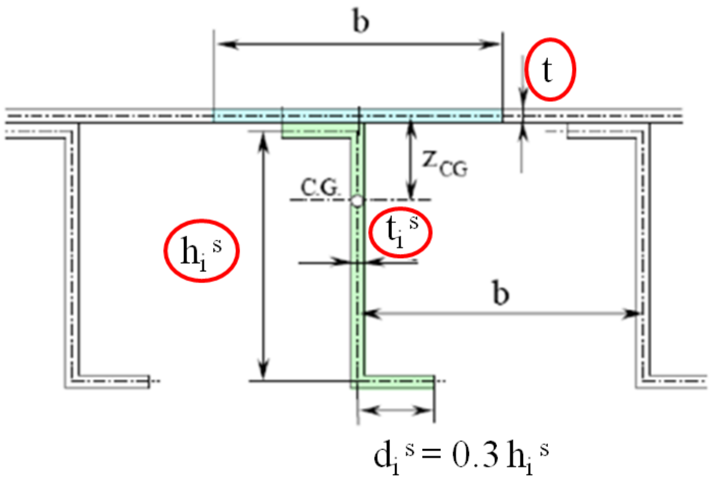

Figure 2: Geometrical design variables of the wing-box stiffened panel.

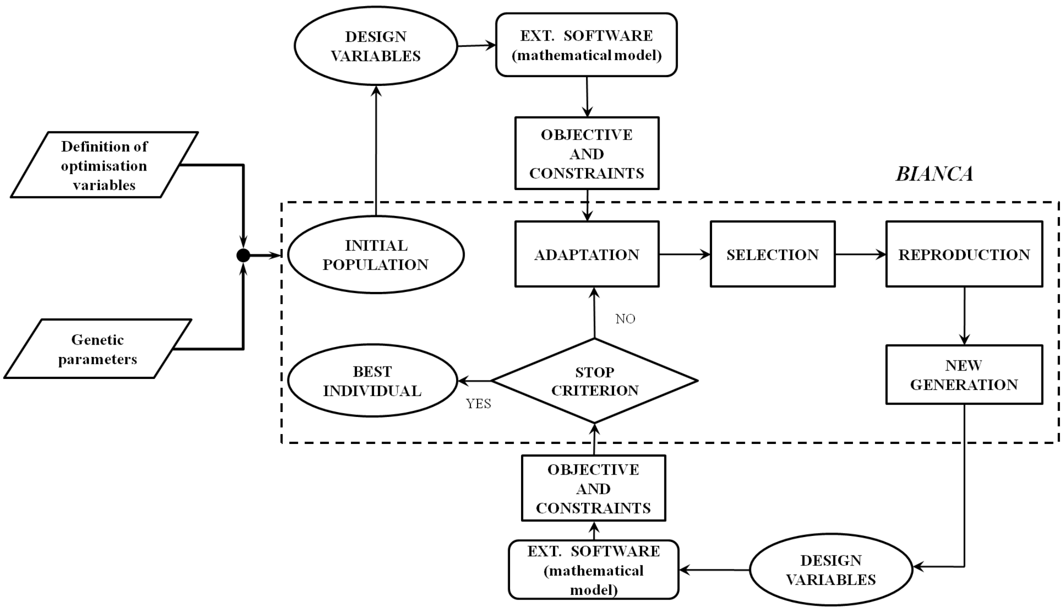

Figure 3: Structure of BIANCA and the interface with external software.

Skin variables	t	R_{0K}^{A*}	R_1^{A*}		
Stiffeners variables	t_1^S	h_1^S	$\left(R_{0K}^{A*}\right)_1^S$	$\left(R_1^{A*}\right)_1^S$	n_r
	t_2^S	h_2^S	$\left(R_{0K}^{A*}\right)_2^S$	$\left(R_1^{A*}\right)_2^S$	
	...	...	...	...	
	$t_{n_r}^S$	$h_{n_r}^S$	$\left(R_{0K}^{A*}\right)_{n_r}^S$	$\left(R_1^{A*}\right)_{n_r}^S$	
	e	e	e	e	

Figure 4: Structure of the individual's genotype for the optimisation problem of the wing-box stiffened panel.

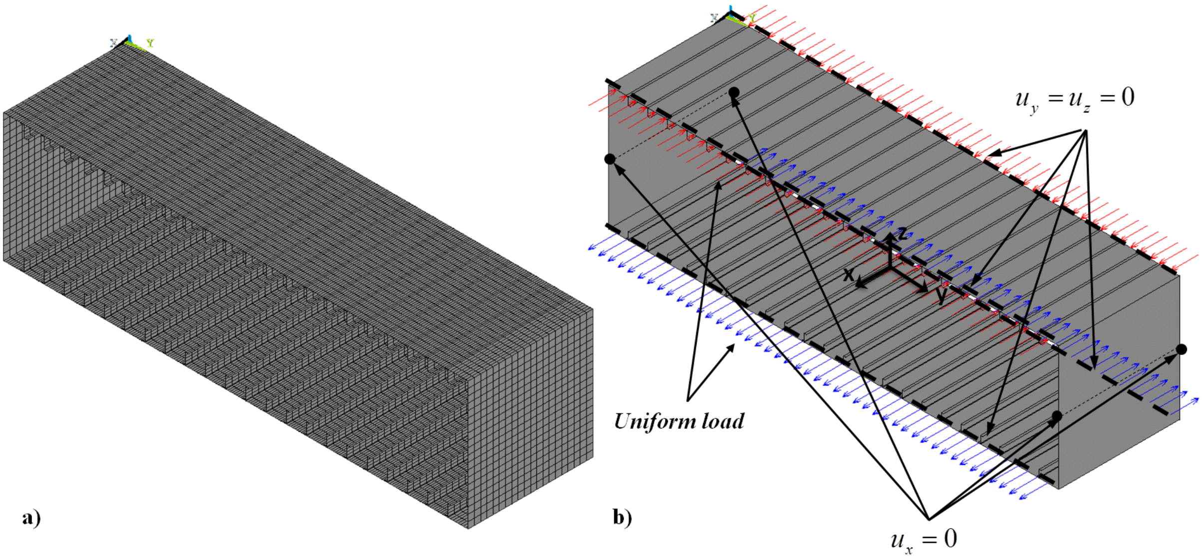

Figure 5: (a) Mesh and (b) loads and boundary conditions for the wing-box FE model.

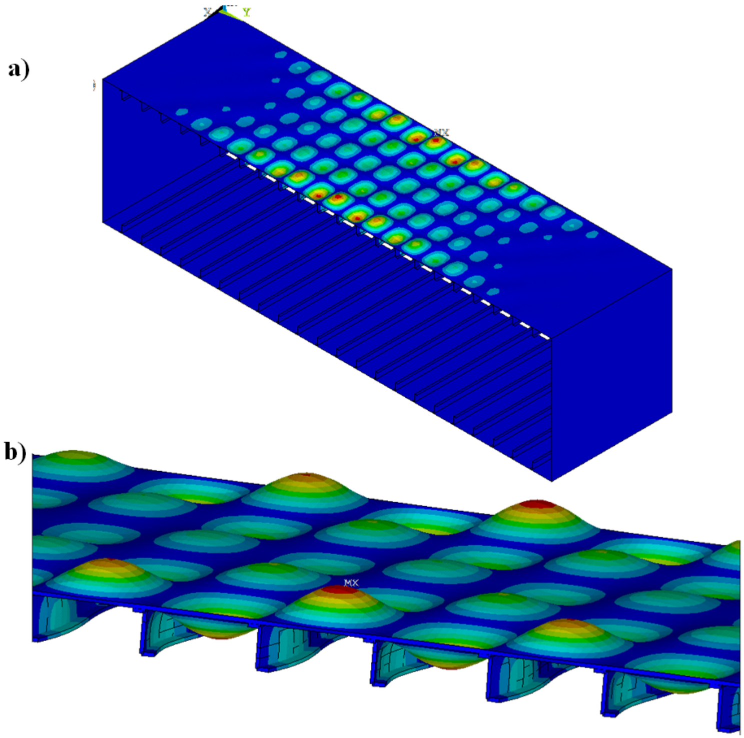

Figure 6: Deformed shape of the a) whole wing-box section and b) upper-panel stiffeners, case with identical stiffeners.

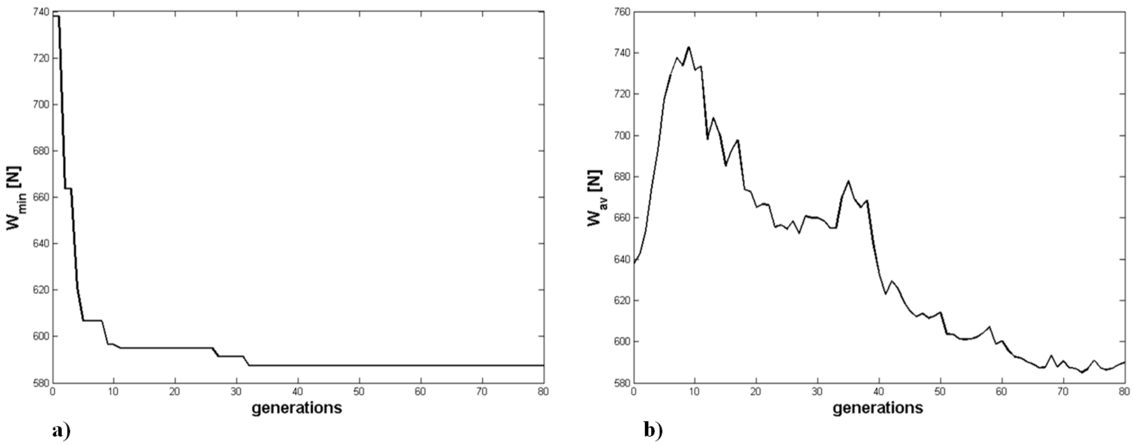

Figure 7: (a) Best and (b) Average values of the objective function along generations for the wing-box FE model, case with identical stiffeners.

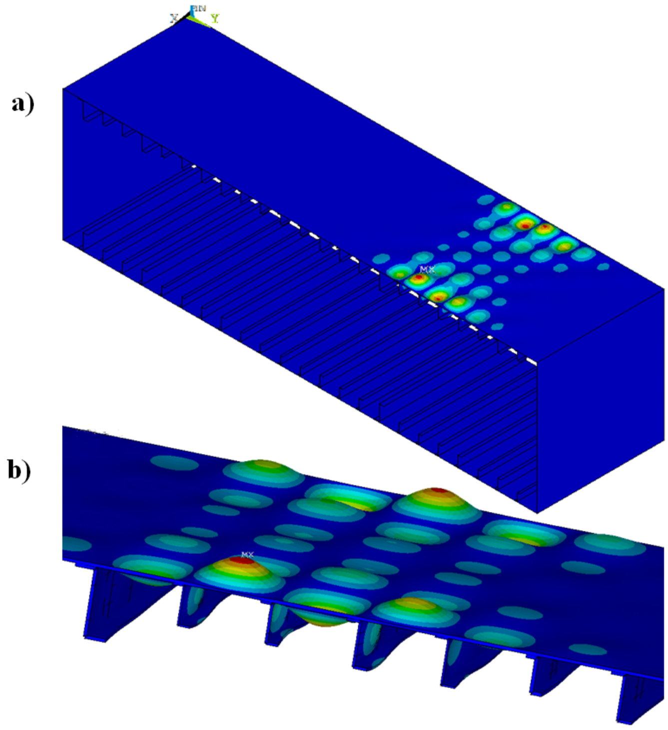

Figure 8: Deformed shape of the a) whole wing-box section and b) upper-panel stiffeners, case with non-identical stiffeners.

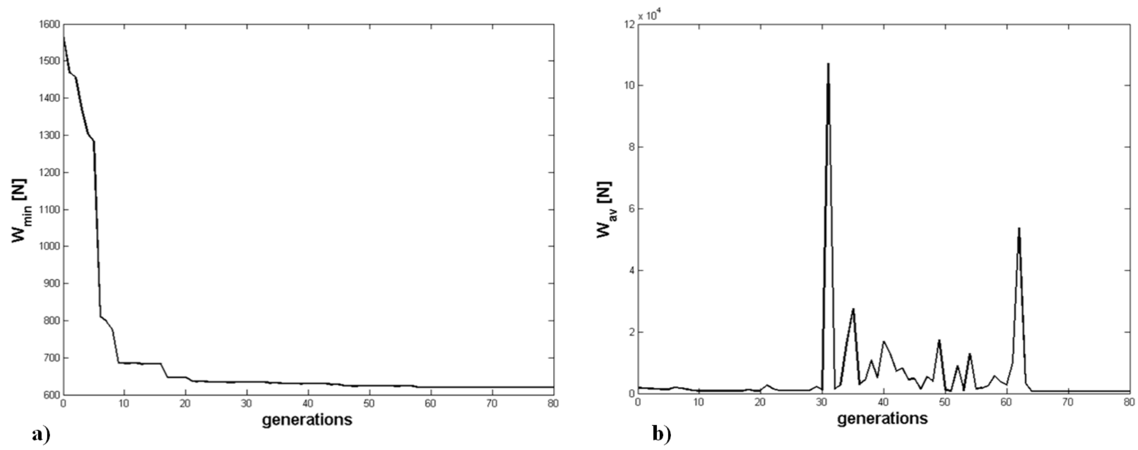

Figure 9: (a) Best and (b) Average values of the objective function along generations for the wing-box FE model, case with non-identical stiffeners.

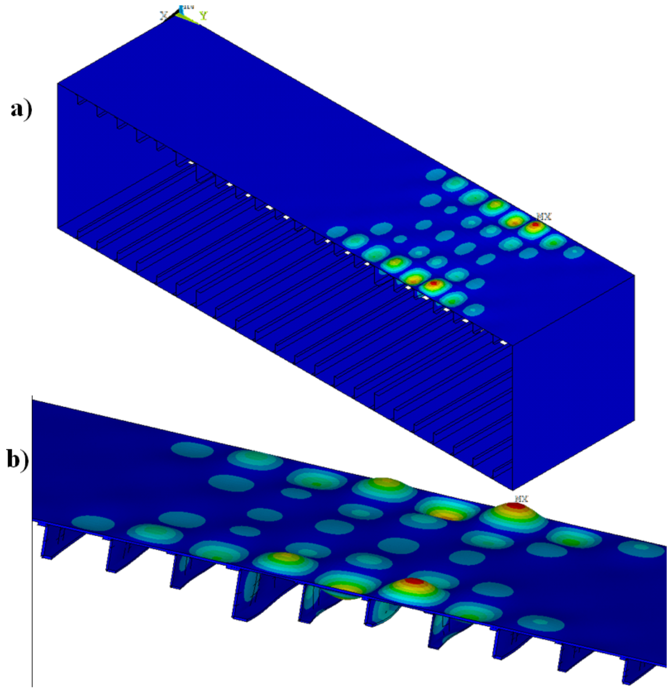

Figure 10: Deformed shape of the a) whole wing-box section and b) upper-panel stiffeners, case with non-identical stiffeners with symmetric distribution.

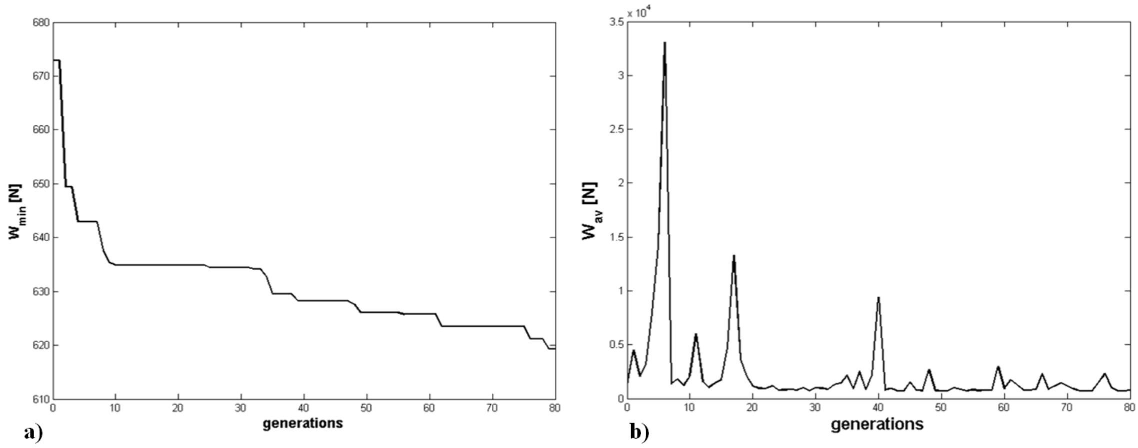

Figure 11: (a) Best and (b) Average values of the objective function along generations for the wing-box FE model, case with non-identical stiffeners with symmetric distribution.